Article:
Kubiak, K orcid.org/0000-0002-6571-2530, Fouvry, S and Marechal, AM (2005) A practical methodology to select fretting palliatives: Application to shot peening, hard chromium and WC-Co coatings. Wear, 259 (1-6). 1. pp. 367-376. ISSN 0043-1648

https://doi.org/10.1016/j.wear.2005.01.030

Published in Wear, Vol. 259, 367 – 376, (2005) – Elsevier http://dx.doi.org/10.1016/j.wear.2005.01.030

A practical methodology to select fretting palliatives: application to shot peening, hard chromium and WC-Co coatings

K.J. Kubiak[1], S. Fouvry[1,], A.M Marechal[2]

[1] *LTDS, CNRS UMR 5513, Ecole Centrale de Lyon,36 Avenue Guy de Collongue, 69134 Ecully, France*

[2] *SNCF, AEF-S, 21, avenue du Président S. Allende 94407 Vitry Sur Seine, France*

krzysztof@kubiak.co.uk

Abstract

Considered as a plague for numerous industrial assemblies, fretting, associated to slight oscillatory displacement, is encountered in all quasi-static contacts subjected to vibration. Depending on sliding conditions, cracking or wear damage can be observed. During the past three decades there has been a huge development in surface treatments. Thousands of new surface treatments and coatings are now available. The critical challenge is to evaluate such treatments against fretting loadings. To achieve this objective, a fast fretting methodology has been developed. It consists in quantifying the palliative friction, cracking and wear responses through a very small number of fretting tests. By defining quantitative variables, a normalized polar fretting damage chart approach is introduced. Applied to shot peening, chromium coatings and WC-Co coatings, it demonstrates the potential benefit of a thermal sprayed WC-Co coating.

Keywords: fretting, fatigue, Cr, WC-Co, friction, cracking, wear.

1. Introduction

Fretting is a slight oscillatory movement, which may occur between contacting surfaces subjected to vibration or cyclic stress. Considered to be very detrimental for modern industry, fretting is encountered in all quasi-static assemblies subjected to vibration, and thus concerns many technologies like helicopters, aircraft, trains, ships, trucks, bridge cables, electrical connections etc … (Fig. 1) [1].

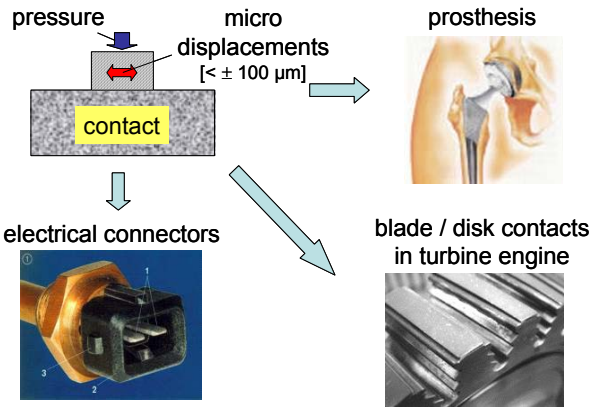

Figure 1 : Illustration of fretting damage.

Partial slip, which is observed for the smallest displacement amplitudes, is characterized by a closed elliptical fretting loop (i.e. evolution of the tangential force (Q) versus the applied displacement (δ) (Fig. 2)). It corresponds to a composite contact displaying sliding and sticking zones. Larger gross slip displacement amplitude conditions, characterized by a quadratic dissipative fretting loop, are related to full sliding conditions. Waterhouse et al. [2] first indicated a correlation between sliding regime and damage evolution (Fig. 2). Cracking has been shown to be mainly observed under the partial slip condition, whereas wear is observed for larger gross slip amplitudes. The damage transition, linked to the displacement amplitude transition (δ_t), is not so sharply marked. However, competitive wear and cracking phenomena are usually observed near this transition. Note that this first description was supported by the fretting map concept first introduced by Vingsbo [3] and completed by Vincent and co-authors [4]. Quantitative approaches have since been developed to formalize either the cracking phenomena from multiaxial fatigue approaches [5-9] or wear kinetics based on a dissipated energy description [8, 10].

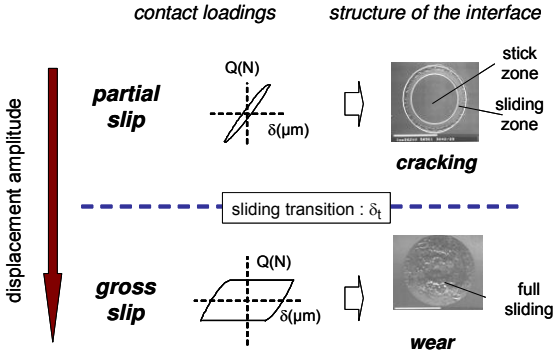

Figure 2 : Illustration of the fretting damage versus the imposed sliding condition.

However, very little has been done to provide a global description of wear and cracking induced by fretting loadings. Even less has been produced regarding a synthetic and complete comparison of palliatives like surface treatments. The purpose of this research is to attempt to answer such a fundamental need by focusing on the two following points:

- The development of a fretting wear test to analyse both wear and cracking induced by fretting through single contact geometry,
- The development of a simplified test methodology to identify the constitutive fretting damage parameters describing fretting behaviours (i.e. friction, wear and cracking).

Applied to a reference 30NiCrMo8/52100 steel contact, this methodology has been extensively used to compare and select several surface treatments like plain shot peening, shot peening + hard chromium electroplating coatings and shot peening + High Velocity Oxy-Fuel (HVOF) WC-Co coatings.

2. Experimental procedure

2.1 Fretting test

As previously mentioned, the applied normal loadings must satisfy the stress conditions, allowing cracking and wear to take place. Displacement control also requires sufficient resolution to cover both partial and gross slip conditions. These two requirements have been satisfied by adapting an original fretting wear test apparatus onto a classical tension-compression (25kN) hydraulic machine already described elsewhere [9]. The contact configuration is presented in Figure 3a.

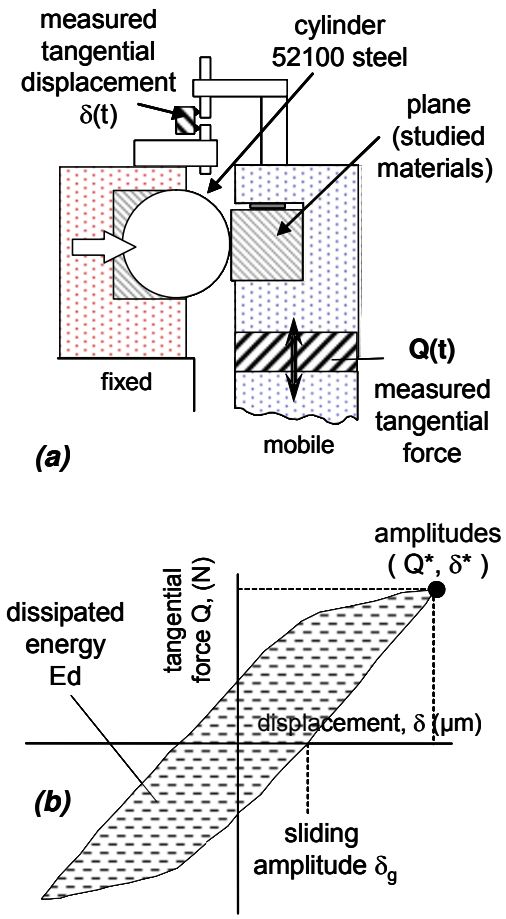

Figure 3 : Test procedure : (a) Fretting setup; (b) Extraction of the contact loading parameters from the fretting loop.

By imposing a 5Hz frequency, the normal force (P) is kept constant while the tangential force (Q) and displacement (δ) are recorded, which permits the plotting of Q-δ fretting loops (Fig. 3b). Thus quantitative variables including the displacement (δ*) and tangential force (Q*) amplitudes, dissipated energy (E_d) and sliding amplitudes (δ_g) can be extracted. The global loading parameters imposed over the test duration like: the average tangential force amplitude,

$$\overline{Q^*} = \frac{1}{N} \cdot \sum_{i=1}^{N} Q^*_i \qquad (1)$$

the cumulated dissipated energy,

$$\Sigma E_d = \sum_{i=1}^{N} E_{di} \qquad (2)$$

and Archard's product of the normal force by the sliding distance:

$$PS = \sum_{i=1}^{N} P_i \cdot 4 \cdot \delta_{gi} \quad (3)$$

can then be calculated.

Prior to testing, all specimens are ultrasonically cleaned first in acetone and then the sliding surfaces are cleaned with ethanol just before contact. All tests are carried out in an ambient laboratory environment (in air, at room temperature), in unlubricated conditions and with relative humidity between 40-50%.

2.2 Studied materials and surface treatments

Substrate and counterbody

Inspired by an industrial application, the studied tribo-couple consists of a low alloy 30NiCrMo8 steel (atomic composition: 0.31% C; 1.06% Mn; 1.1 %Cr; 0.79 %Ni) used as the substrate for surface treatments fretted against a 52100 steel. The 30NiCrMo8 steel was machined to 10x10x15 mm square cubes and polished on one side to a very low surface roughness (R_a < 0.05 µm). A similar surface roughness was measured on the 40 mm radius 52100 AISI steel cylinder counterbody. To verify plane strain conditions, the contact length (L) was fixed at 5 mm inducing an a/L ratio below 0.1 (i.e. a: half width of the Hertzian contact). The studied 30NiCrMo8 steel was heat treated at 820°C, oil quenched (20°C) and temperate at 520±5 ºC for 2 hours to obtain the mechanical properties listed in Table 1.

Table 1 : Mechanical properties of the steel involved in the fretting analysis.

	52100 (counterbody)	30NiCrMo (substrate)
Elastic modulus, E (GPa)	210	200
Poisson ratio, ν	0.29	0.3
Yield stress, σ_{Y02} (MPa)	1700	740
Maximum stress, σ_R (MPa)	2000	890

Studied Surface Treatments

Three classical surface treatments, extensively applied against fretting damage, have been investigated.

Shot peening

Shot peening, applied to all the coated substrates, was conducted following the conventional procedure of 0.0063A (200% recovering and balls of 0.6 mm diameter). Carried out on an air blast machine it satisfies the MIL-S-13165 standard, equivalent to an ALMEN intensity of 0.2-0.3 mm. The average roughness of the specimens was R_a=2 µm.

Shot peening + WC-Co HVOF coating

A tungsten carbide thermal spray coating was applied to the shot peened specimens, using a HP/HVOF process. A WC-17% Cobalt powder was used to reach a 140 µm coating thickness. An average surface roughness R_a=0.1 µm was measured on the coated and polished surfaces.

Shot peening + hard chromium electroplating

As above, a set of shot peened specimens was selected for hard chromium deposition. A conventional electroplating process was carried out using a chromic acid solution with 250g/l of CrO_3, with a current density from 31 to 46 A/dm^2. An average coating thickness of 220 µm was obtained with a surface roughness R_a equal to 0.2 µm after polishing.

2.3 Procedure of damage quantification

Crack length quantification

Because fretting wear stressing alone can not propagate the crack until the flat specimen ruptures, cracking is analysed by measuring and comparing the crack length below the surface as a function of the loading conditions. The following assessment procedure has been applied (Fig. 4a): The plane specimen on which the fretting test was performed is precisely cut perpendicularly across the middle of the fretting scar. After careful polishing, optical cross section observations are made to measure the position and the length of the deepest crack (l_{max}). Note that crack orientation and multi-cracking activation are highly dependent on the imposed partial slip condition [12].

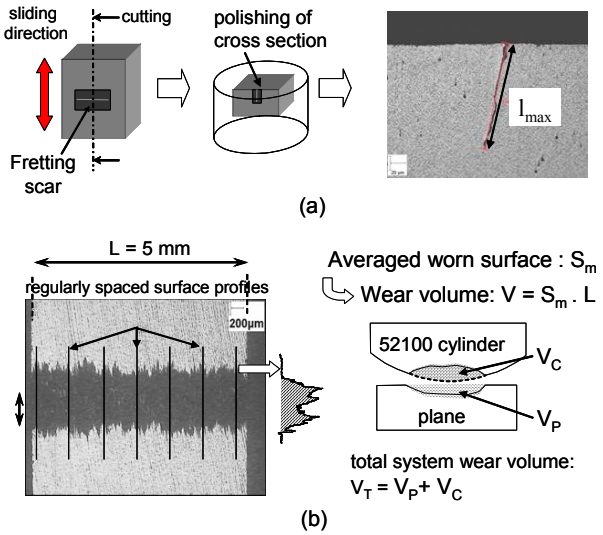

Figure 4 : (a) Fretting crack assessment (partial slip test conditions); (b) Wear volume estimation (gross slip test conditions).

Wear volume measurement

One advantage of the 2D cylinder / plane configuration is that the wear volume can be estimated from a limited number of low cost 2D surface profiles (Fig. 4b). The following procedure was applied: First, the specimens were ultrasonically cleaned to eliminate as much debris as possible. Several regularly-spaced surface profiles, perpendicular to the fretting scar, were then made. An average fretting wear surface was then computed which, multiplied by the contact length (L), allowed the plane wear volume (V_P) to be estimated. Note that previous comparison with complete 3D surface profiles has confirmed a wear volume dispersion which was lower than 7 %. The wear volume of the counter-body (V_C) was similarly defined by extracting the cylinder shape from the surface profiles. Finally, the total wear volume of the fretting contact was estimated:

$$V_T = V_P + V_C \qquad (4)$$

3. Development of experimental methodology

3.1 Definition of the contact conditions

Expertises in the field of Tribology and Fatigue have shown that the closer the test configurations to the industrial application, the finer the palliative endurance predictions. This condition of similitude is presently illustrated by analysing an axle-pressed fitted assembly.

Precise FEM modeling was first undertaken to extract the real contact pressure field distribution. Due to the extreme loading range and the complexity of the contact configuration (i.e. a symmetrical peak pressure distribution was identified), such an industrial configuration can not be reproduced for the available test. However in order to capture the contact stress severity, the chosen cylinder/plane configuration was adjusted to reproduce as closely as possible the external peak pressure. This was achieved by applying a constant 2000 N normal force which provides a representative p_0=600 MPa maximum peak pressure and an equivalent a=430 µm half contact width (Fig. 5). If FEM computations can provide reasonable contact pressure estimations of the distributions, predicting the relative displacements is more difficult. A simple strategy is to cover a sufficient range of displacements in order to first identify the partial/gross slip transition, to quantify the cracking phenomena under partial slip condition and finally to compare the wear activated under gross slip (Fig. 6) [9].

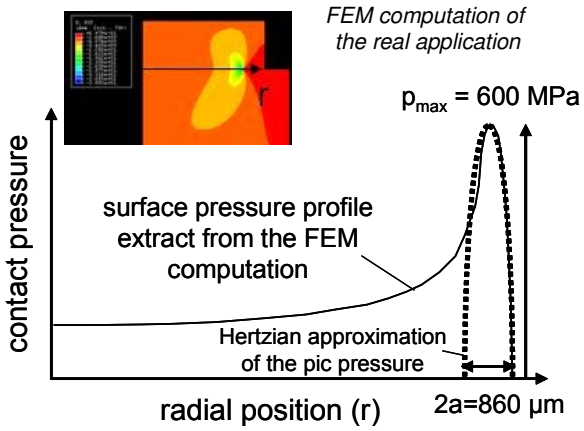

Figure 5 : Illustration of the methodology to identify representative Hertzian loading conditions.

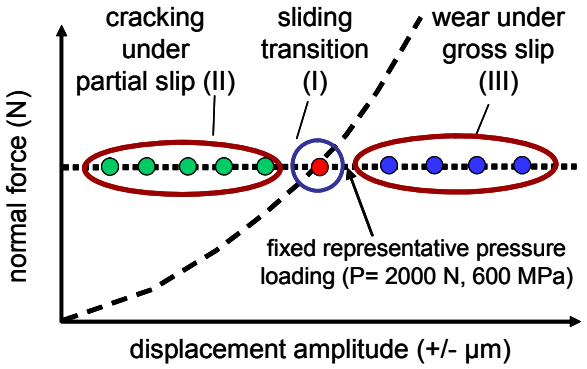

cracking analysis under partial slip (II) (250 10^3 cycles)	PS/GS sliding transition (I) (Q_t, δ_t)	wear analysis under gross slip (III) (25 10^3 cycles)
tangential force control: Q^* (± N): Q_{th} – 0.9 Q_t (5 tests)	variable sliding test	displacement control: δ^* (± µm): 25,50,75,100 (4 tests)

Figure 6 : Definition of the fretting test methodology (R=40 mm, L=5mm, f=5Hz).

3.2 Fretting sliding analysis and identification of pertinent friction parameters

To identify the displacement amplitude marking the transition from partial to gross slip sliding conditions, an incremental displacement methodology has been adapted [11]. Very slight displacement amplitude is imposed at the beginning and increased in regular steps. Hence, through a single fretting test, a complete overview of the sliding response is provided. Note that the consistency of this methodology is fully dependent on the incremental displacement step ($\Delta\delta$) and the chosen number of fretting cycles imposed to stabilize the sliding contact (ΔN) during the increment (Fig. 7a). Previous investigations have shown that perfect coherence with classical constant sliding test conditions is achieved if the incremental increase of the sliding amplitude remains smaller than $\Delta\delta$=0.2 µm and the stabilized period above ΔN=1000 cycles. Figure 7b illustrates the reference 30NiCrMo8/52100 contact response. The normalized tangential force ratio (Q/P) as well as the dissipated energy criterion $A = Ed/(4.Q^*.\delta^*)$ are plotted versus the applied displacement amplitude. The sliding transition (δ_t) from partial to gross slip is related to an energy discontinuity confirming Mindlin's formalism. This discontinuity is associated to a maximum value of the tangential force amplitude also related to the friction coefficient at the sliding transition (μ_t) (i.e. representative of the friction coefficient operating under partial slip conditions [8]).

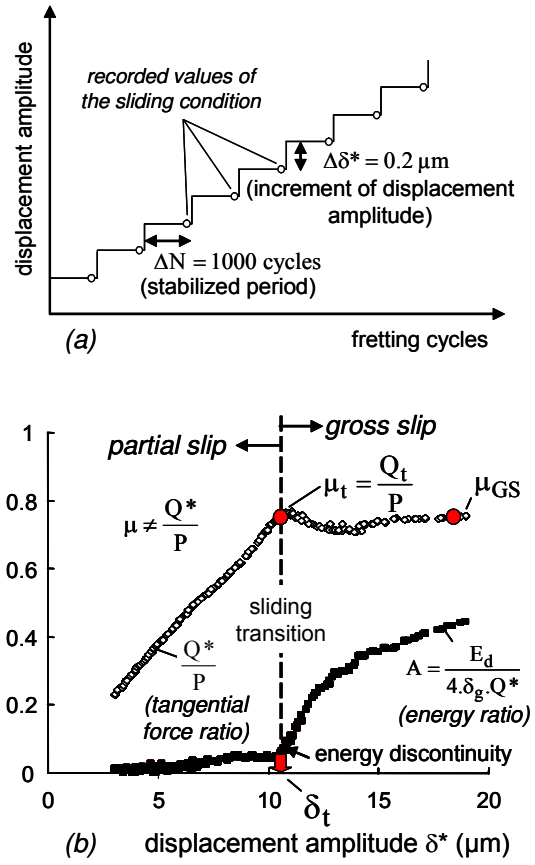

Figure 7 : Illustration of the incremental sliding method: (a) definition of the procedure; (b) application to the 30NiCrMo8/52100 contact: identification of the sliding transition (δ_t), the coefficient of friction at the sliding transition (μ_t) and the friction coefficient under stabilized gross slip conditions (μ_{GS}).

Above the sliding transition, the full sliding conditions, by favouring wear, generates a compliant interfacial third body and promotes a decrease of the friction coefficient. A stabilized friction value, representative of the friction law under gross slip conditions is then identified (μ_{GS}). The quantitative variables (δ_t, μ_t, μ_{GS} Q_t) defining the tribological behaviour of the studied tribosystems are compiled in Table 2 and illustrated in Figure 8. Smaller frictions values are identified well under gross slip conditions. Moreover, smaller fluctuations can be observed for the coated contacts. Displaying dissimilar material composition, they limit the adhesion phenomena and provide more stable friction performances. As previously outlined [12] no significant differences can be observed between the plain and peened surfaces. Moreover, the decrease of the friction coefficient induced by the two studied

coatings is quite limited. A hard chromium coating seems to induce smaller friction coefficients (0.6 – 0.7) but the difference is not significant and can not be compared with the drastic modification induced by the application of low friction lubricant coatings [13, 14].

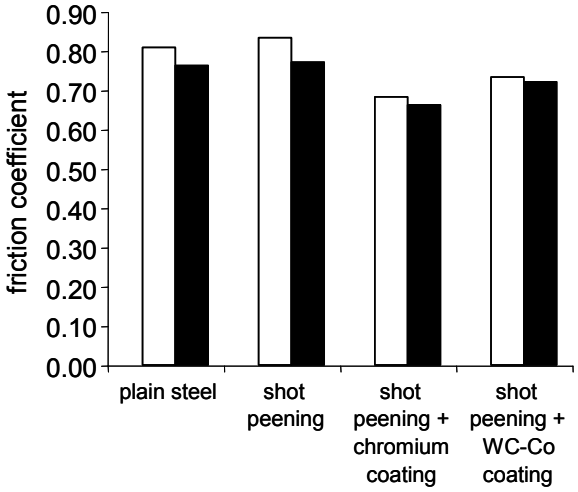

Figure 8 : Comparison of the studied mean friction coefficients defined from the incremental sliding analysis: □ friction coefficient defined at the sliding transition (μ_t), ■ friction coefficient defined under stabilized gross slip conditions (μ_{GS}).

Table 2: Synthesis of the various fretting parameters extracted from the given fretting methodology to quantify respectively friction behaviour, cracking responses under stabilized partial slip and wear kinetics under gross slip conditions.

Surface treatment	μ_t ratio	μ_{GS} ratio	Q_t N	δ_t µm
plain steel	0.81	0.76	1615	16.4
shot peening	0.83	0.77	1669	15.6
shot peening + chromium coating	0.68	0.66	1378	13.6
shot peening + WC-Co coating	0.73	0.72	1469	10.4

Surface treatment	P N	Q_{th} N	l_{MAX}(µm)	[$Q \approx 0.9 \cdot Q_t$(N)]
plain steel	2005	1090	103	1480
shot peening	1997	1100	47	1490
shot peening + chromium coating	2000	0(1)	223	1290

shot peening + WC-Co coating	2002	1490(2)	0	1290

(1) The value is associated to zero because the crack nucleation threshold of such a coating can not be detected by this fretting test apparatus.

(2) No crack has been detected even when applying the highest cyclic loading conditions (i.e. sliding transition) for the studied pressure field. Hence the crack nucleation threshold is associated to this maximum possible loading state.

Surface treatment	Archard wear coefficient K			Energy wear coefficient α(μm³/J)		
	$K_{TREAT.}$ μm³/Nm	K_{52100} μm³/Nm	K_{TOTAL} μm³/Nm	$\alpha_{TREAT.}$ μm³/J	α_{52100} μm³/J	α_{TOTAL} μm³/J
plain steel (reference)	8481	9650	18132	14534	16372	30906
shot peening	11689	4943	16632	18738	7936	26674
shot peening + chromium coating	1602	8949	10552	2581	14416	11834
shot peening + WC-Co coating	550	1407	1957	920	2356	3276

3.3 Analysis of the fretting cracking under partial slip conditions

Figure 9 illustrates the methodology to quantify the cracking response under partial slip. The maximum crack length is achieved at the maximum tangential loading close to the sliding transition. Above this sliding transition the reduction of the friction coefficient and a competitive effect of wear tend to reduce the crack extension [2, 8]. To investigate a crack, constant tangential force amplitudes are applied by properly adjusting the partial slip displacement amplitude. Previous analysis has shown that the crack arrest condition is reached after a test duration of around 250 000 cycles.

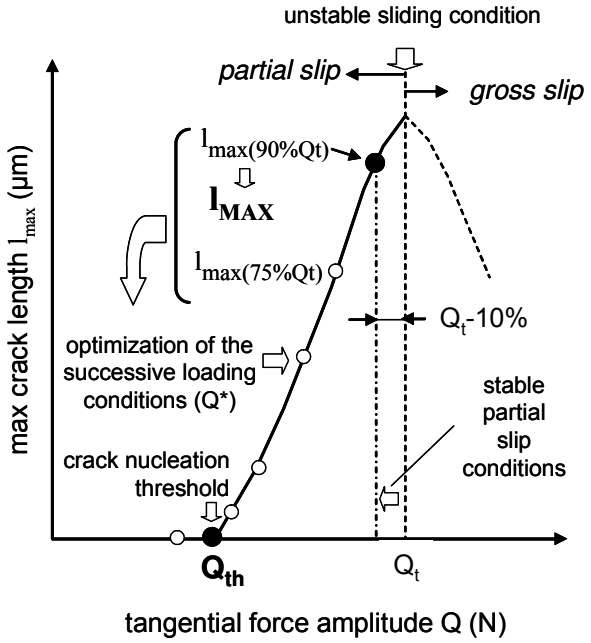

Figure 9 : Illustration of the simplified fretting cracking methodology: identification of the basic cracking parameters (crack nucleation threshold: Q_{th}; fretting crack propagation behaviour: $l_{MAX}=l_{max(90\%Qt)}$).

To maintain stable partial slip conditions, the first fretting test is adjusted to tangential force amplitude slightly below the transition value (0.9 Q_t). A second test is conducted around 75% of the transition amplitude. By comparing the corresponding maximum crack lengths, the successive test conditions are adjusted to fully describe the crack length evolution versus the tangential force amplitude and to bracket as precisely as possible the threshold crack nucleation (Q_{th}). Therefore in 4 to 6 fretting tests, two quantitative variables defining the contact crack nucleation and crack extension can be extracted.

- The threshold crack nucleation tangential force amplitude (Q_{th})
- The maximum crack length is defined at 90% of the maximum tangential force amplitude and is obviously related to the maximum crack length of the fretting contact for the studied pressure condition: $l_{MAX}=l_{max(90\%Qt)}$. The various tribo-systems have been investigated and the corresponding parameters are compiled in Table 2.

Figure 10 compares crack length evolution versus the applied tangential force amplitude. Considering the limited number of fretting tests, linear approximations have been applied to describe cracking evolution. The reference plain 30NiCrMo8 steel presents a crack nucleation threshold Q_{th} close to 1100 N and tends to propagate up to a maximum crack length l_{MAX}

close to 110 µm. Such treatment does not improve crack nucleation resistance but is a significant benefit regarding propagation.

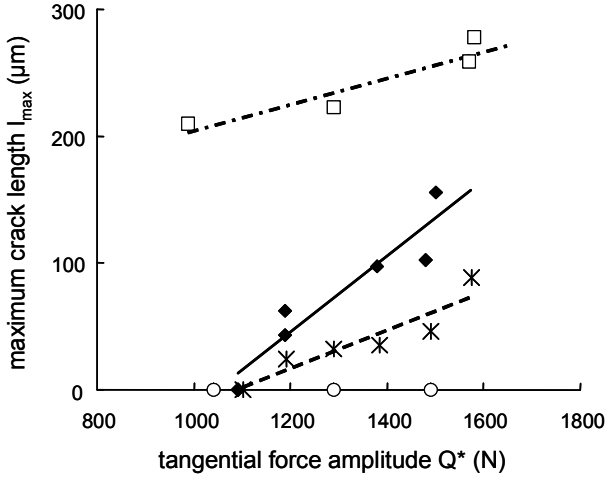

Figure 10 : Evolution of the crack length versus the applied tangential force amplitude (◆: reference plain 30NiCrMo8 steel; ✳: shot peening; □: shot peening + chromium coating; ○: shot peening + WC-Co coating).

To interpret such behaviour it is essential to consider the very sharp stress gradient imposed below the fretting contact. The cumulated cyclic plastic strain, which is at maximum on the top surface, tends to rapidly relax the initial compressive stresses introduced by the treatment. Hence the potential beneficial impact of shot peening on the surface crack nucleation is rapidly erased. When the crack extends below the surface, crossing domains less affected by contact loading, a higher compressive stress state are maintained which consequently decreases the propagation rate. The chromium coating cracking results also confirm previous fatigue investigations [15]. Due its very brittle behaviour, very slight contact loading will immediately activate coating cracking. Hence, even for loading conditions lower than the reference crack nucleation threshold, crack lengths equivalent to the coating thickness can be detected. This confirms the very detrimental effect of such treatment on fretting cracking and more particularly on the incipient nucleation stage. However the substrate crack propagation rate appears smaller than for the plain material. Two hypotheses can be made to explain this evolution:

First, the application of a thick coating protects the substrate from the maximum surface stress. It consequently decreases the corresponding crack tip stress intensity factors and

promotes smaller crack kinetics. On the other hand, to compare the different cracking rates it is essential to consider similar crack lengths and calculate representative stress intensity factors. This complex problem involving complete and difficult crack modeling of the coated contact can not be addressed in the present work.

The second hypothesis concerns the positive impact of the initial peening treatment. Protected from relaxation phenomena by the coating thickness, the compressive stress fields are maintained, which limits crack propagation through the substrate.

These two hypotheses are probably true. However, different cross section observations showing vertical coating cracks which are inclined when they propagate through the substrate tends to support the second hypothesis (Fig. 11).

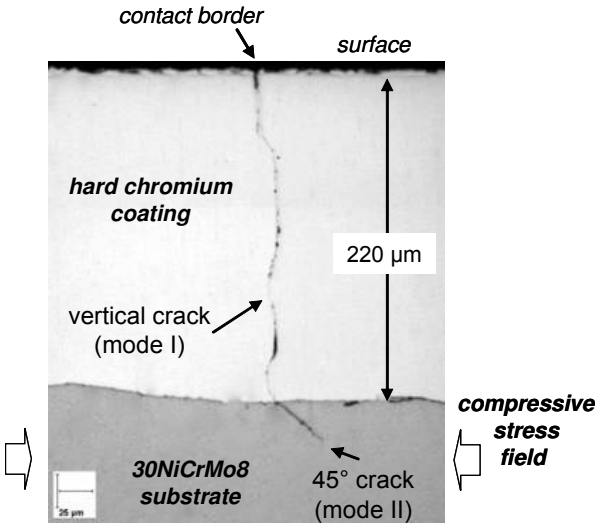

Figure 11 : Typical evolution of the shot peening + chromium coating fretting cracking behavior (p_0=600 MPa, Q*=1580 N).

The chromium coating is very brittle which can explain the initial mode I controlled vertical crack. Conversely, the 45° orientation observed through the substrate can only be explained by very high compressive states maintained just below the coating interface. They impose severe crack closure conditions and only permit a less efficient shear mode II propagation regime. The conclusion is that the chromium coating is very detrimental at the fretting crack nucleation stage, and this demonstrates the need to systematically apply prior shot peening treatment to limit the substrate propagation rate at least.

The analysis of WC-Co shows that no crack nucleations were activated within the studied loading conditions. This methodology such a treatment appears to be the best fretting cracking palliative studied according to this methodology. However, more in depth analyses, including fretting fatigue tests, are required to fully evaluate its crack propagation performance.

3.4 Quantification of wear under gross slip.

To compare the wear behaviour under gross slip, four displacement amplitudes from ±25 to ± 100 µm were applied (Fig. 12). Compared to the cracking phenomena the wear steady state is reached after a few thousand cycles, so the test duration can be reduced to 25000 cycles.

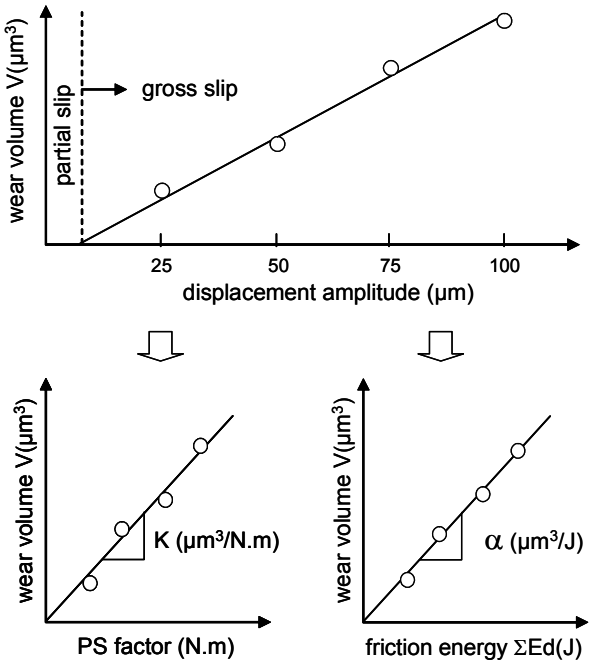

Figure 12 : Illustration of the methodology applied to quantify wear under gross slip conditions.

For the first approximation the Archard model, (i.e. wear volume versus the PS product) [16], can be applied. A linear approximation is extrapolated to extract the slope of the wear kinetics, also defined as Archard's wear coefficient:

$$K\left(\mu m^3 / Nm\right) = \frac{\Delta V}{\Delta PS} \qquad (5)$$

Recent studies show that an energy approach displays higher stability [17]. This model compares the wear volume to the friction energy dissipated through the interface (ΣE_d). The

impact of the friction coefficient is thus better taken into consideration. Linear evolutions are classically observed, allowing the energy wear coefficient to be identified:

$$\alpha\left(\mu m^3 / Nm\right) = \frac{\Delta V}{\Delta \Sigma E_d} \qquad (6)$$

To interpret the various wear mechanisms and more particularly the transfer phenomena, the plane, the cylinder but also the total wear system will be analysed. It is interesting to highlight the intrinsic differences between these two formulations. The energy description rationalizes the wear damage extension as a function of the energy driven through the interface. It allows more fundamental investigations by relating for instance the wear damage processes to thermodynamical concepts [17]. The Archard analysis, which is a more practical approach, associates the wear kinetics to the main contact loadings imposed on the contact: the normal force and the sliding distance. Note that under stable friction behaviours, like those observed in the present study, the two Archard and Energy formulations are proportional and justify the fact that this analysis mainly focuses on the energy description.

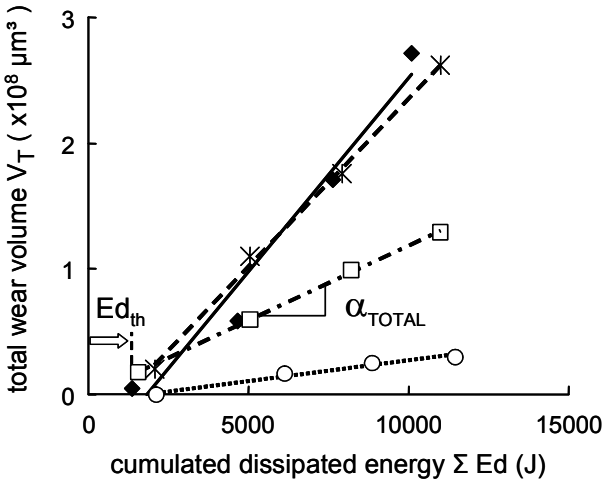

Figure 13 : Evolution of the total wear volume increase versus the cumulated dissipated fretting energy: (◆: reference plain 30NiCrMo8 steel ; ✳: shot peening; □: shot peening + chromium coating; ○: shot peening + WC-Co coating).

Figure 13 confirms the linear increase of the system wear volume versus the cumulated dissipated energy. However this linear evolution does not cross the origin but presents a slight shift along the energy axis associated to wear incubation threshold energy (Ed_{th}). Previous research [17] has shown that this energy can be related to the cumulated plastic transformation first required to modify the initial microstructure to a very hard phase, the so-

called Tribologically Transformed Structure TTS. This very brittle structure is successively fractured and generates the incipient wear debris. All the studied tribosystems involve metallic materials, which promote similar threshold energies. Therefore, the studied wear palliatives can be analysed directly by comparing the energy and Archard's wear coefficients (Table 2). The comparison in terms of system or total wear resistance indicates that the shot peening treatment has absolutely no impact on wear resistance. The chromium coating performs rather well, with an energy wear coefficient half that of the reference. Again the best performance is observed for the WC-Co coating with an energy wear coefficient at least 9 times lower than the reference system. Figure 14 and Table 2, by compiling the different wear energy and Archard's coefficients, allow the comparison of flat and cylinder counterbodies. The reference 30NiCrMo8/52100 contact displays quasi homogeneous wear between the first two first bodies. More interesting is the 30NiCrMo8 + shot peening/52100 response. The plastic deformation induced by peening treatment was supposed to increase the surface hardness of the flat surface and possibly increase the wear resistance. The reverse situation is in fact observed. To interpret this behavior the brittleness of the plastic transform surface and the introduction of numerous micro cracks generated during the peening treatment should be mentioned. The observed higher relative wear kinetics of the peened surface can then be explained. More complete investigations are however necessary to confirm and better quantify this aspect.

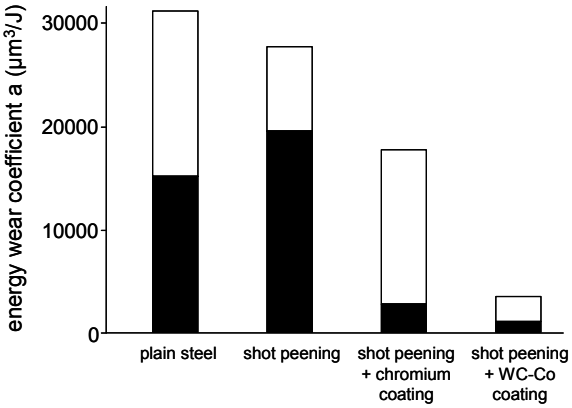

Figure 14 : Wear kinetics of the studied tribosystems (Energy wear approach): □ : α_{52100} cylinder counterbody, ■: $\alpha_{TREAT.}$ studied surface treatment (plane), □+■: α_{TOTAL} whole contact.

The chromium coating displays sharper differences. The wear kinetics of the chromium is very low whereas the wear of the 52100 steel is quasi identical to the reference. It appears that most of the wear is in fact generated on the steel counterbody which explains factor two, previously outlined during the total wear analysis. Fundamental research, focusing on the 52100 steel transfers onto the chromium coating should be undertaken to explain such a heterogeneous wear response. The WC-Co/52100 tribosystem displays homogeneous and low wear kinetics. The intrinsic wear resistance of the WC-Co is not significantly different from the chromium. The main gain is in fact related to a drastic drop of the 52100 wear kinetics. The advantage of the WC-Co coating is that in addition to providing very low system wear kinetics, it generates homogeneous and stable wear kinetics of the two counterparts. This could be of fundamental interest for the maintenance procedures of industrial assemblies.

4. Synthesis and conclusion

Tables 2 compiles the different parameters extracted from this simplified fretting damage methodology. It permits a quantitative comparison of the different aspects associated to fretting damage such as friction behaviour under partial and gross slip conditions, cracking phenomena during the nucleation and propagation stages, and finally wear under gross slip situations. To provide a synthetic illustration of the palliative's performance, an optimized fretting damage chart is introduced. The respective performance of palliatives is normalized versus the reference system in such a way that the calculated ratio is below one if the treatment is beneficial or above 1 if it is detrimental. The following variables are considered:

Fretting tribological properties:

$$\underline{\mu_t} = \frac{\mu_t}{\mu_t(\mathrm{ref})},\ \underline{\mu_{GS}} = \frac{\mu_{GS}}{\mu_{GS}(\mathrm{ref})},\ \underline{Q_t} = \frac{Q_t}{Q_t(\mathrm{ref})},\ \underline{\delta_t} = \frac{\delta_t}{\delta_t(\mathrm{ref})}, \tag{7}$$

Fretting cracking properties:

$$\text{Nucleation: } \underline{Q_{th}} = \frac{Q_{th}}{Q_{th}(\mathrm{ref})}, \text{ Propagation } \underline{l_{MAX}} = \frac{l_{MAX}}{l_{MAX}(\mathrm{ref})}, \tag{8}$$

Fretting wear properties:

$$\underline{\alpha_{TOTAL}} = \frac{\alpha_{TOTAL}}{\alpha_{TOTAL}(\mathrm{ref})},\ \underline{\alpha_{52100}} = \frac{\alpha_{52100}}{\alpha_{52100}(\mathrm{ref})},\ \underline{\alpha_{TREAT.}} = \frac{\alpha_{TREAT.}}{\alpha_{TREAT.}(\mathrm{ref})}, \tag{9}$$

$$\underline{K_{TOTAL}} = \frac{K_{TOTAL}}{K_{TOTAL}(\mathrm{ref})},\ \underline{K_{52100}} = \frac{K_{52100}}{K_{52100}(\mathrm{ref})},\ \underline{K_{TREAT.}} = \frac{K_{TREAT.}}{K_{TREAT.}(\mathrm{ref})}, \tag{10}$$

Different plots can be applied, the polar representation, first introduced by Carton and co-authors [18] for fretting analysis, is user-friendly. It is here extended and normalised to compare the studied surface treatment responses (Fig. 15).

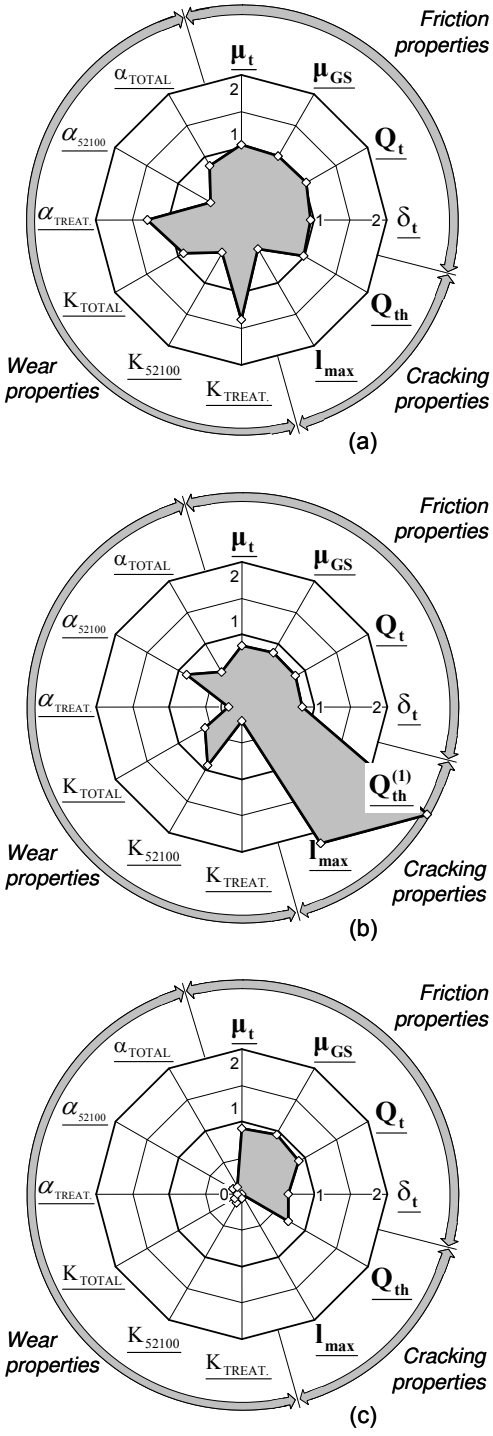

Figure 15 : Development of a normalized polar representation to compare the different fretting palliative responses (reference system: 30NiCrMo8/52100 contact) (a) shot peening treatment, (b) shot peening + chromium coating, (c) shot peening + WC-Co coating.

A rapid overview shows that the peening treatment does not modify friction behaviour, does not change the crack nucleation response but increases crack propagation resistance. Wear resistance is little changed but there are differences between coated (plane) and uncoated (cylinder) surfaces. The chromium coating slightly decreases the friction coefficients but it is very detrimental regarding cracking response. It decreases the system wear kinetics but displays a very heterogeneous response. Finally the WC-Co coating characterized by slightly lower friction behaviour displays very good cracking performance and presents very low and homogeneous wear kinetics. This quick methodology demonstrates the potential interest of applying a thermal spray WC-Co coating against fretting damage. However, if these results are important for industrial applications, many restrictions must be considered. The present study was conducted under dry conditions [19]. In numerous cases, lubricants are applied, and this aspect requires a specific investigation. This analysis is also restricted to constant sliding conditions whereas most real applications undergo variable and complex loadings. Synergy damage phenomena can operate during combined partial and gross slip sliding which again requires specific analyses [17]. This research has been conducted for plain contact loading without introducing external stressing. Indeed, these results must be carefully interpreted and specific precautions must be taken before extending such a classification to any different stressing situations.

To conclude, this fretting palliative selection method appears to be a convenient way to compare various surface treatments, particularly when a wide range of surface treatments are potentially interesting. However it cannot replace the complete investigation required for a definitive validation for an industrial implementation. These two approaches are not competitive but fully complementary: the fast methodology can be conducted to operate a first selection among a wide range of possible palliatives whereas classical fretting and fretting fatigue analyses must be performed to validate a choice through a restricted number of solutions.

References

[1] Hoeppner D. "Mechanisms of fretting fatigue and their impact on test methods development", ASTM STP 1159, 1992, p. 23-32.

[2] Waterhouse R.B., "Fretting Fatigue", R.B. Waterhouse (Ed.), Applied Science, London, 1981.

[3] Vingsbo O., Soderberg. S. "On fretting Maps" Wear 126, 1988, p. 131-147.

[4] Vincent L. "Materials and Fretting", Fretting Fatigue, ESIS 18, 1994, p.323-337.

[5] McVeigh P.A., Farris T. N., "Finite element analysis of Fretting Stresses", Journal of Tribology, 119, 1997, p. 797-801.

[6] Araujo J. A., Nowell D., "The effect of rapidly varying contact stress fields on fretting fatigue", International Journal of Fatigue, 24, 2002, p. 763-775.

[7] Vallellano C., Dominguez J., Navarro A., "On the estimation of fatigue failure under fretting conditions using notch methodologies", Fatigue Fract. Eng., M26 (5), 2003, p. 469-478.

[8] Fouvry S., Kapsa Ph., Vincent L., "Quantification of fretting damage", Wear 200, 1996, p. 186-205.

[9] Fouvry S., Duo P., Perruchaut Ph. "A quantitative approach of Ti-6Al-4V fretting damage: Friction, Wear and crack nucleation ",Wear 257, issue 9-10, 2004,p. 916-929.

[10] Mohrbacher H., Blanpain B., Celis J.P., Roos J.R., " Oxidational wear of TiN coating on tool steel and nitrided tool steel in unlubricated fretting", Wear, 180, 1995, p. 43-52.

[11] Voisin J. M., Vannes A. B., Vincent L., Daviot J., Giraud B., "Analysis of a tube-grid oscillatory contact: methodology for the selection of superficial treatments", Wear, 181-183, 1995, p. 826-832.

[12] Fridrici V., Fouvry S., Kapsa Ph.,"Effect of shot peening on the fretting wear of Ti-Al-4V", Wear 250, 2001, p. 642-649.

[13] Fridrici V., Fouvry S., Kapsa Ph., Perruchaut Ph. "Impact of contact size and geometry on the lifetime of a solid lubricant ", Wear 255, 2003, p. 875-882.

[14] Zhou Z R, Vincent L. "Lubrification in Fretting a review", Wear 225-229, 1999, p. 962-967.

[15] Nascimento M. P., Souza R. C., Pigatin W. L., Voorwald H. J. C. ,"Effects of surface treatments on the fatigue strength of AISI 4340 aeronautical steel", International Journal of Fatigue, Vol. 23, Issue 7, 2001, p.607-618.

[16] Archard J., "Contact and rubbing of flat surfaces", Appl. Phys., 24, 1953, p. 981-988.

[17] Fouvry S., Liskiewicz T., Kapsa Ph., Hannel S., Sauger S., " An energy description of wear mechanisms and its applications to oscillating sliding contacts", Wear 255, 2003, p. 287-298.

[18] Carton J. -F., Vannes A. B., Vincent L., "Basis of a coating choice methodology in fretting", Wear, 185, 1995, p.47-57.

[19] McColl I R, Waterhouse R.B., Harris S.J., Tsujikawa M., "Lubricated fretting wear of high-strength eutectoid steel rope wire", Wear 185, 1995, p. 203-212.